p27BBP/eIF6 acts as an anti-apoptotic factor upstream of Bcl-2 during *Xenopus laevis* development

N De Marco[1], L Iannone[2], R Carotenuto[1], S Biffo[3,4], A Vitale[5] and C Campanella*,[1]

p27BBP/eIF6 (β4-binding protein/eukaryotic initiation factor 6) regulates the joining of 40S and 60S ribosomal subunits, on receptor for activated C kinase 1 binding and protein kinase C phosphorylation in serine 235. In *Xenopus*, p27BBP/eIF6 is abundantly expressed in the majority of the embryonic anlagen. Although p27BBP/eIF6 abundance may be required for a general regulation of protein synthesis, our data suggest that p27BBP/eIF6 may target the translation of specific mRNAs. We injected Xp27BBP/eIF6 mRNA in one blastomere of two-cell-stage embryos and obtained a bent phenotype, the curvature being lateral with respect to the embryo antero-posterior axis. The injected side had fewer apoptotic cells than the uninjected side, whereas cell proliferation appeared unaffected. Accordingly, in Xp27BBP/eIF6 morphants, endogenous apoptosis increased. Injection of Xp27BBP/eIF6 point mutants indicated that the anti-apoptotic action of Xp27BBP/eIF6 requires the conserved S235. The bent phenotype was also obtained with B-cell lymphoma gene-2 (Bcl-2) overexpression and was rescued by Bcl-2-associated X protein (Bax)/Xp27BBP/eIF6 co-injection. In addition, embryos overexpressing Xp27BBP/eIF6 had a higher amount of Bcl-2 and an unchanged amount of Bax with respect to controls. In Xp27BBP/eIF6 morphants, Bcl-2 levels were unaffected and Bax levels were higher than in the controls. Thus, we propose that Xp27BBP/eIF6 is part of a mechanism acting on the specific translation of messengers regulating cell survival. In particular, we suggest that Xp27BBP/eIF6 may regulate the translation of factors upstream of Bcl-2/Bax.
Cell Death and Differentiation (2010) **17,** 360–372; doi:10.1038/cdd.2009.128; published online 25 September 2009

Protein p27BBP/eIF6 (β4-binding protein/eukaryotic initiation factor 6) is a highly conserved regulator of ribosomal function. It regulates the binding of 40S and 60S ribosomal subunits [1] and is necessary for the biogenesis of 60S and cell growth in organisms as diverse as yeast[2–4] and mammals.[5] In the latter, p27BBP/eIF6 null mice are lethal before implantation, whereas heterozygous mice, which present 50% reduction of p27BBP/eIF6 levels in all tissues, show a decrease in body mass.[5] p27BBP/eIF6, when bound to 60S, act as factors preventing 40S and 60S subunits from joining in the 80S assemblage. The assemblage of 80S is regulated by Efl1p in yeast cells [3] and by receptor for activated C kinase 1 (RACK1)/protein kinase C (PKC) signaling in mammals. In particular, in mammalian cells, on PKC phosphorylation of serine 235, p27BBP/eIF6 is released from 60S to start translation.[6] Accordingly, a serine phosphorylated isoform of p27BBP/eIF6 has been found in *Xenopus laevis*,[7] in which two potential PKC phosphorylation sites have been found, that is, 235 SmR in common with mammals and 91SvR specific to *X. laevis*.[8,9]

Although p27BBP/eIF6 is an essential gene,[10] its expression is variable. p27BBP/eIF6 mRNA and protein levels are high in rapidly proliferating tumoral cells and low in cells committed to apoptosis.[11] In normal mammalian tissues, p27BBP/eIF6 levels are variable among cell types, suggesting that *in vivo* its expression is tightly regulated.[10,12]

During *Xenopus* embryogenesis, chains of induction bring to the construction of the body anlagen through proliferation, apoptosis and differentiation. In this system, a modulated expression of p27BBP/eIF6 occurs in developing anlagen in addition to a basal level of expression. In particular, p27BBP/eIF6 mRNA is abundant in the eye field and in the mid-hindbrain boundary, two regions with high proliferation levels.[8,9] Recently, the study of p27BBP/eIF6 has gained new interest because this protein seems to regulate the translation of specific mRNAs such as β-catenin mRNA, thus modulating the fundamental signaling of the Wnt/β-catenin pathway.[13] Moreover, it has been proposed that p27BBP/eIF6 functions in miRNA-mediated post-transcriptional silencing because it is part of RNA-induced silencing complex (RISC)

[1]Department of Structural and Functional Biology, University of Naples Federico II, Naples, Italy; [2]AMRA Center of Competence, University of Naples Federico II, Naples, Italy; [3]Department of Science and Advanced Technology, University of Eastern Piedmont, 'Amedeo Avogadro', Alessandria, Italy; [4]DIBIT and University Vita-Salute San Raffaele Milan, Milan, Italy and [5]TIGEM, Naples, Italy
*Corresponding author: C Campanella, Department of Structural and Functional Biology, University of Naples Federico II, Naples, Italy.
Tel: + 39 081 679200; Fax: + 39 081 679233; E-mail: chiara.campanella@unina.it

Abbreviations: A-P, antero-posterior axis; Bax, Bcl-2-associated X protein; Bcl-2, B-cell lymphoma gene-2; BrdU, 5-bromo-2′-deoxyuridine; BSA, bovine serum albumin; D-V, dorsoventral axis; DAPI, 4′-6-diamidino-2-phenylindole; DTT, dithiothreitol; e, eye; EGTA, ethylene glycol tetraacetic acid; enc, encephalon; end., endoderm; GFP, green fluorescent protein; H, head; HEPES, *N*-2-hydroxyethylpiperazine-*N*′-2-ethanesulfonic acid; HUA, hydroxyurea and aphidicolin; i.s, injected side; m, miotome; mo, morpholino; nc, notochord; ot.v, otic vesicle; p27BBP/eIF6, β4-binding protein/eukaryotic initiation factor 6; PARP, poly (ADP-ribose) polymerase; PBS, phosphate-buffered saline; ph, pharynx; pH3, phospho histone 3; PKC, protein kinase C; RACK1, receptor for activated C kinase 1; SBTI, soybean trypsin inhibitor; SDS-PAGE, SDS-polyacrylamide gel electrophoresis; sp.c., spinal cord; RT-PCR, reverse transcriptase-PCR; T, tail; TAME, *N*α-(*p*-toluene sulfonyl)-L-arginine methyl ester; Tris, hydroxymethyl aminomethane

and as such, in *Caenorhabditis elegans*, it specifically represses the translation of LIN-14 and LIN-28 mRNAs without an effect on the general translation.[14] In other experimental systems, p27[BBP]/eIF6 is not necessary for miRNA-based translational repression.[15] To reveal whether p27[BBP]/eIF6 has a qualitative role in gene expression, we studied the effects of ectopic overexpression of p27[BBP]/eIF6 in *X. laevis* development

The analysis of a mutated phenotype stemming out from our study has highlighted a novel function for p27[BBP]/eIF6: its potential role as an apoptosis inhibitor. Apoptosis is physiologically required for normal development during *Xenopus* embryogenesis, where it occurs with a reproducible pattern, starting from late gastrulation.[16] In addition to its general role in controlling the cell number in developing anlagen, apoptosis participates in the process of neural determination,[17] and is essential for several processes including the removal of the tail in anurans during metamorphosis and of the interdigital membrane in the developing vertebrate limb.[18] Here, we show that p27[BBP]/eIF6 although overexpression does not induce an increase in cell number, it does induce a decrease in apoptotic nuclei. A similar effect is seen by B-cell lymphoma gene-2 (Bcl-2) overexpression.

p27[BBP]/eIF6 overexpressing embryos showed an increase of Bcl-2 that was not found in p27[BBP]/eIF6 morphants. In addition, although p27[BBP]/eIF6 overexpression did not modify the levels of Bcl-2-associated X protein (Bax) expression, in the morphants, Bax mRNA and protein levels are higher than in the controls, suggesting that p27[BBP]/eIF6 may be upstream in the same apoptotic pathway. Moreover, the S235A p27[BBP]/eIF6 mutant lacked an anti-apoptotic function, indicating that S235A is the site responsible for this function and suggesting that the anti-apoptotic role of p27[BBP]/eIF6 relies on its ribosome anti-associative function.

Results

p27[BBP]/eIF6 overexpression causes bending of the embryo.

We injected Xp27[BBP]/eIF6 mRNA (from 100 pg to 500 pg) together with green fluorescent protein (GFP) mRNA (300 pg) in one blastomere of the two-cell-stage *X. laevis* embryos to investigate the effects of its overexpression. Given that the first cleavage plane divides the embryo in two symmetrical halves, in these experiments the uninjected side can be considered as the natural control of each test. Xp27[BBP]/eIF6 expression was controlled by immuno-fluorescence or western blot analysis with a specific anti-p27[BBP]/eIF6 antibody and consistently indicated that the injected part was expressing more protein as opposed to the uninjected part (Figure 1). Two days after injection, about 40% of st.28 embryos showed a marked bending lateral with respect to the antero-posterior axis of the embryo and the embryos became ring-shaped. The external, concave side derived from the injected blastomere, as this side was marked by GFP fluorescence ($n = 80$) (Figures 2a–c). This phenotype was transient and recovered at stage 35.

Control experiments showed that the single injection of GFP mRNA at the concentration described above did not produce bent embryos or defective phenotypes (see Figure 2a). When Xp27[BBP]/eIF6 mRNA was injected before cleavage, at one-cell stage, no bending occurred in st.28 embryos (Figures 2d and e), indicating that the bent phenotype occurs when the mRNA is injected only on one side of the embryo. Previous data have shown that the endogenous Xp27[BBP]/eIF6 is abundantly expressed in somites.[8,9] Accordingly, to investigate whether the bending might be due to defects of number, position or dimension of the somite metameric pattern, we performed whole-mount immunohistochemistry using an antibody directed against the myotome protein 12/101, a somite marker. No difference or defect was observed in the somites between the injected and the control side (Figure 2f), suggesting that the bent phenotype was because of an unbalanced number of cells with respect to the embryo symmetry plane.

p27[BBP]/eIF6 overexpression does not increase proliferation.

As Xp27[BBP]/eIF6 is particularly abundant in territories showing high proliferation,[8,9] we asked ourselves whether p27[BBP]/eIF6 overexpression causes an increase in cell number on the injected side. First, we counted the nuclei number in 4′-6-diamidino-2-phenylindole (DAPI)-stained p27[BBP]/eIF6 overexpressors. In Figures 3a–d, counts were performed in serial sections of embryos ($n = 15$, $P < 0.05$), in areas of 3000 μ^2 settled through the Leica, Wetzlar, Germany, Laser Microdissection LMD V6.5 software. The number of cells was higher on the side of injection compared with the uninjected side (Figure 3d), whereas in embryos injected with GFP alone ($n = 15$, $P < 0.05$), there was no difference between the number of nuclei counted on the injected and uninjected sides of the embryo (Figure 3e–h).

The embryos injected with Xp27[BBP]/eIF6 were then tested for 5-bromo-2′-deoxyuridine (BrdU) incorporation. At 2 h after BdrU injection (see Viczian *et al.*[19]), the embryos were fixed and cryostat-sectioned. We further stained the serial sections with antibodies against BrdU or phospho histone 3 (pH3), markers of mitotic cells. No difference was detected in BrdU-positive cells on the injected side compared with the uninjected side (Figures 3j). Counts of pH3-positive nuclei in embryos entirely sectioned showed no significant difference in the number of cycling cells between the control and injected side ($n = 30$, $P < 0.05$) (Figure 3k and l). Taken together, these results suggest that p27[BBP]/eIF6 overexpression does not lead to an increase of cells in the S phase. Therefore, the observed increase in cell numbers leading to the bent phenotype may be due to differences in the cell survival rates on the two sides of the embryo, rather than proliferation.

Overexpression of p27[BBP]/eIF6 reduced endogenous apoptosis in embryos.

During *Xenopus* development, apoptosis is first detected at gastrulation and later in development, during the tailbud stage when it is found in the developing brain, eyes, spinal cord and tail.[20] The TUNEL assay has proved to be effective and specific for detecting apoptosis in *Xenopus* embryos[16,20] as in other systems.[21] We thus compared the incidence of TUNEL-positive nuclei on the side of the embryos overexpressing p27[BBP]/eIF6 compared with the control side. The labeled apoptotic nuclei were largely on the control side, whereas the injected side showed little apoptosis, as observed in whole-mount
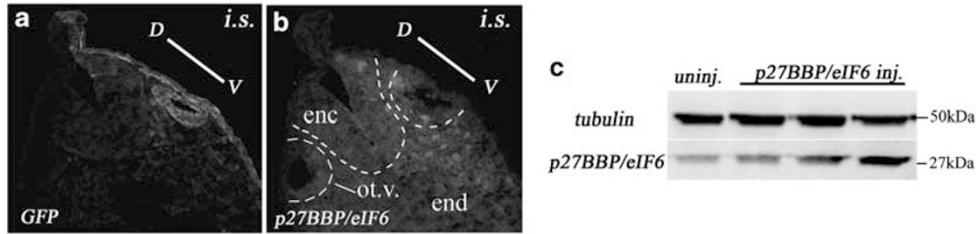
Figure 1 Xp27[BBP]/eIF6 overexpression. In serial cross-sections of Xp27[BBP]/eIF6 and GFP-injected embryos, the injected side is immunostained with anti-GFP (**a**) and with anti-p27[BBP]/eIF6 antibodies (**b**). In the latter case, the lower level of immunostaining is on the uninjected side indicating the w.t. expression of Xp27[BBP]/eIF6. enc, encephalon; ot.v, otic vesicle; end, endoderm. (**c**) Western blot with anti-p27[BBP]/eIF6 antibody indicates the major presence of protein in p27[BBP]/eIF6-injected embryos with respect to uninjected embryos. Three sets of injected embryos were used in the blot. Normalization was performed with anti-α-tubulin antibody. D-V, dorsoventral axis. The injected side is indicated (i.s)
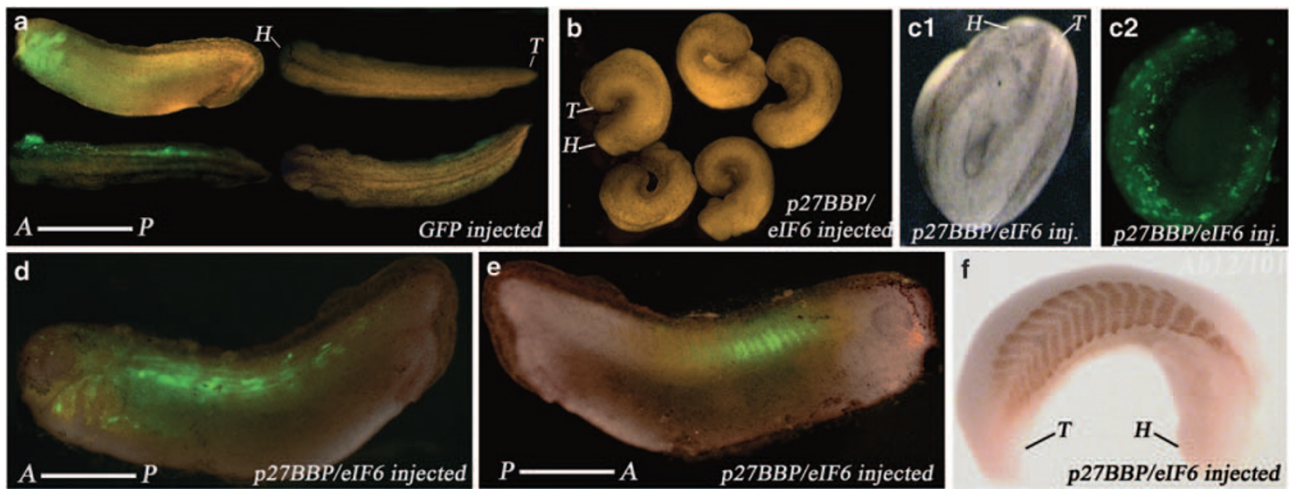
Figure 2 Effects of Xp27[BBP]/eIF6 overexpression. Compared with GFP-injected embryos (**a**) (lateral and dorsal view), 40% of the Xp27[BBP]/eIF6 overexpressing embryos showed a bent phenotype at st.28 (**b**), the side deriving from the injected blastomere being the external and concave side (**c1**) marked by GFP fluorescence (**c2**). When Xp27[BBP]/eIF6 injection was performed at one-cell stage (**d–e**), no bending occurred in the embryos, suggesting that the bent phenotype occurs when Xp27[BBP]/eIF6 is overexpressed only on one side of the embryos. Micrographs of the two sides (**d–e**) of the same embryo are given. Whole-mount immunohistochemistry with 12/101 antibody showed no defects in size, number and morphology of the somite metameric pattern (**f**). H, head; T, tail; D-V, dorsoventral axis

embryos and related sections (Figures 4a and b). We made counts of TUNEL-positive nuclei in sections of injected embryos fixed at stage st.28 and entirely sectioned (Figures 4c and d). We found a significantly lower percentage of apoptotic nuclei on the Xp27[BBP]/eIF6-injected side compared with the control side ($n = 30$, $P < 0.05$) (Figure 4e). We did not see differences in control embryos, either uninjected or injected uniquely with GFP mRNA ($n = 15$, $P < 0.05$) (Figure 4f).

Caspase 3 is a polypeptide of 32 kDa that releases an active peptide of 18 kDa on cleavage.[22] During apoptosis, the 116 kDa form of the poly (ADP-ribose) polymerase (PARP1) is cleaved to form a peptide of 85 kDa.[23] We carried out western blots to analyze the executioner caspase 3 and PARP1 cleavage. Xp27[BBP]/eIF6-injected embryos showed less active caspase 3 and more uncleaved PARP1 than did uninjected or GFP-injected embryos (Figure 4g and h).

These results indicate that Xp27[BBP]/eIF6 overexpression exerts an anti-apoptotic action contrasting the physiologically occurring apoptosis during *X. laevis* embryogenesis.

We further checked whether p27[BBP]/eIF6 downregulation of apoptosis depended on cell cycling, by treating the injected embryos with hydroxyurea and aphidicolin (HUA), which inhibits DNA synthesis in the early S phase of the cell cycle.[24] Despite the decline in cell proliferation as shown by anti-pH3 staining of HUA-treated embryos, we observed a decrease in the number of apoptotic cells on the side overexpressing Xp27[BBP]/eIF6 (Figures 5a–c). We conclude that the anti-apoptotic effect of Xp27[BBP]/eIF6 is independent of cell cycling.

Downregulation of Xp27[BBP]/eIF6 increases endogenous apoptosis. We injected Xp27[BBP]/eIF6 morpholino (7.5 ng) together with GFP mRNA (200 pg) in one blastomere of a two-cell-stage *X. laevis* embryos to investigate the effects of p27[BBP]/eIF6 downregulation. As a control, a mispaired morpholino (7.5 ng) was injected together with GFP mRNA (200 pg) to distinguish the specific effects of Xp27[BBP]/eIF6 morpholino injection. The p27[BBP]/eIF6 downregulation was monitored by immunofluorescence or western blot analysis with the anti-p27[BBP]/eIF6 antibody (data not shown).
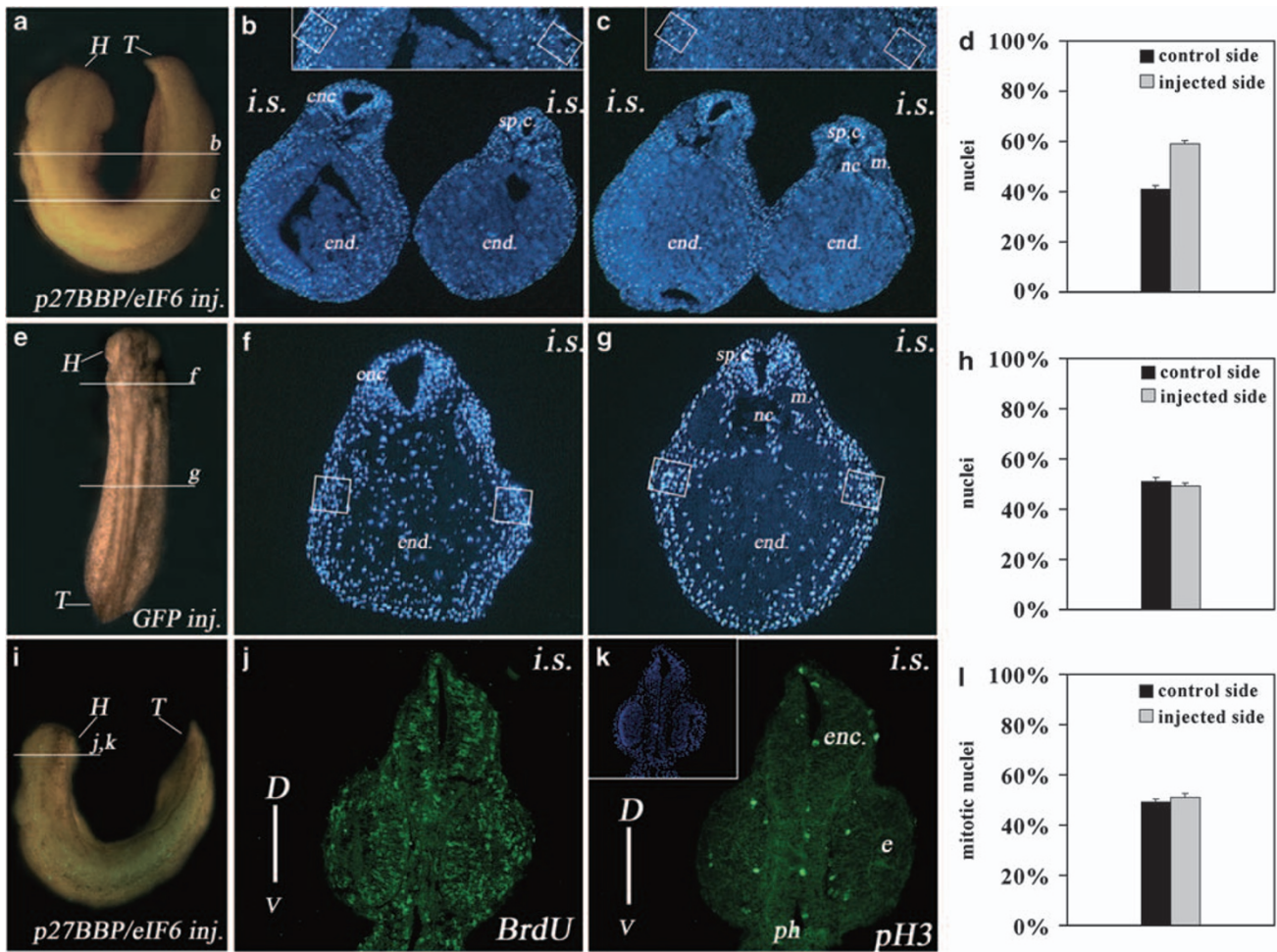
Figure 3 Proliferation assays on Xp27[BBP]/eIF6 overexpressing embryos. DAPI staining was carried out in bent embryos overexpressing Xp27[BBP]/eIF6 (**a–c**). Panels **b** and **c** show embryo sections cut as shown in **a**. DAPI-stained nuclei were counted in 3000 μ^2 areas, as indicated in panels **b** and **c** insets. The nuclei number is higher on the injected side than on the uninjected side (**d**). The counts are statistically significant ($n = 15$, $P < 0.05$). (**e–g**) DAPI staining in embryos injected uniquely with GFP. Counts of nuclei in sections cut as shown in (**e**) indicate no differences in cell number between the uninjected and the GFP-injected side (**h**) ($n = 15$, $P < 0.05$). (**i–l**) Panels **j** and **k** are sections of Xp27[BBP]/eIF6 overexpressors cut as shown in (**i**). (**j–k**) Immunolocalization with anti-BrdU and anti-pH3 antibodies on the serial section of an Xp27[BBP]/eIF6-overexpressing embryo (injected with BrdU at st.28). No difference was detected in BrdU- or pH3-positive cells (**k**) on the injected side, compared with cells of the uninjected side. Nuclei are contrasted with DAPI (inset in **k**). (**l**) Counts of pH3-positive nuclei on a section of Xp27[BBP]/eIF6-overexpressing embryos showed no difference in cells in mitosis between the injected and control sides ($n = 30$, $P < 0.05$). D-V, dorsoventral axis. The injected side is indicated (i.s). enc, encephalon; e, eye; ph, pharynx; sp.c., spinal cord; nc, notochord; end., endoderm; m, miotome

Although the morpholino control injection did not produce defective phenotypes (Figure 6a), about 50% of st.28 morpholino-injected embryos showed a bent phenotype symmetrical to the phenotype obtained by Xp27[BBP]/eIF6 overexpression, as the embryos were bent with the concave, external side opposite to the injected side (Figure 6b). TUNEL assay showed a major percentage of apoptotic nuclei on the morpholino-injected side compared with the uninjected one ($n = 20$, $P < 0.05$) (Figures 6c,d and g), thus confirming the anti-apoptotic role of Xp27[BBP]/eIF6.

In eIF6^{+/−} adult mice, specific organs, that is, the liver and fat body, display reduction of cell proliferation.[5] Thus, we asked whether in Xp27[BBP]/eIF6 morphants a general decrease in cell proliferation could be observed. Data show that embryos injected with Xp27[BBP]/eIF6 morpholino and GFP on the one side and with mispaired morpholino

(Figures 6e and f) on the opposite side had no differences in the number of anti-pH3-positive nuclei ($n = 20$, $P < 0.05$) (Figure 6h). It should be noted, however, that specific counts in hepatocytes and fat cells could not be performed in adult *Xenopus* to parallel the eIF6^{+/−} mice observations.[5] Indeed, in *Xenopus* embryos, liver cells differentiate at stage 46,[25] when the bent phenotype had recovered and fat cells appear following metamorphosis (see Rot-Nikcevic and Wassersug[26]).

S235A mutant loses the anti-apoptotic function. *X. laevis* p27[BBP]/eIF6 cDNA has two serine embedded in a PKC consensus phosphorylation site: one is serine 235 and is conserved in mammals, and the other is serine 91 and is typical of *Xenopus*.[8,9] In mammalian cells, translation occurs when p27[BBP]/eIF6 is released from 60S following
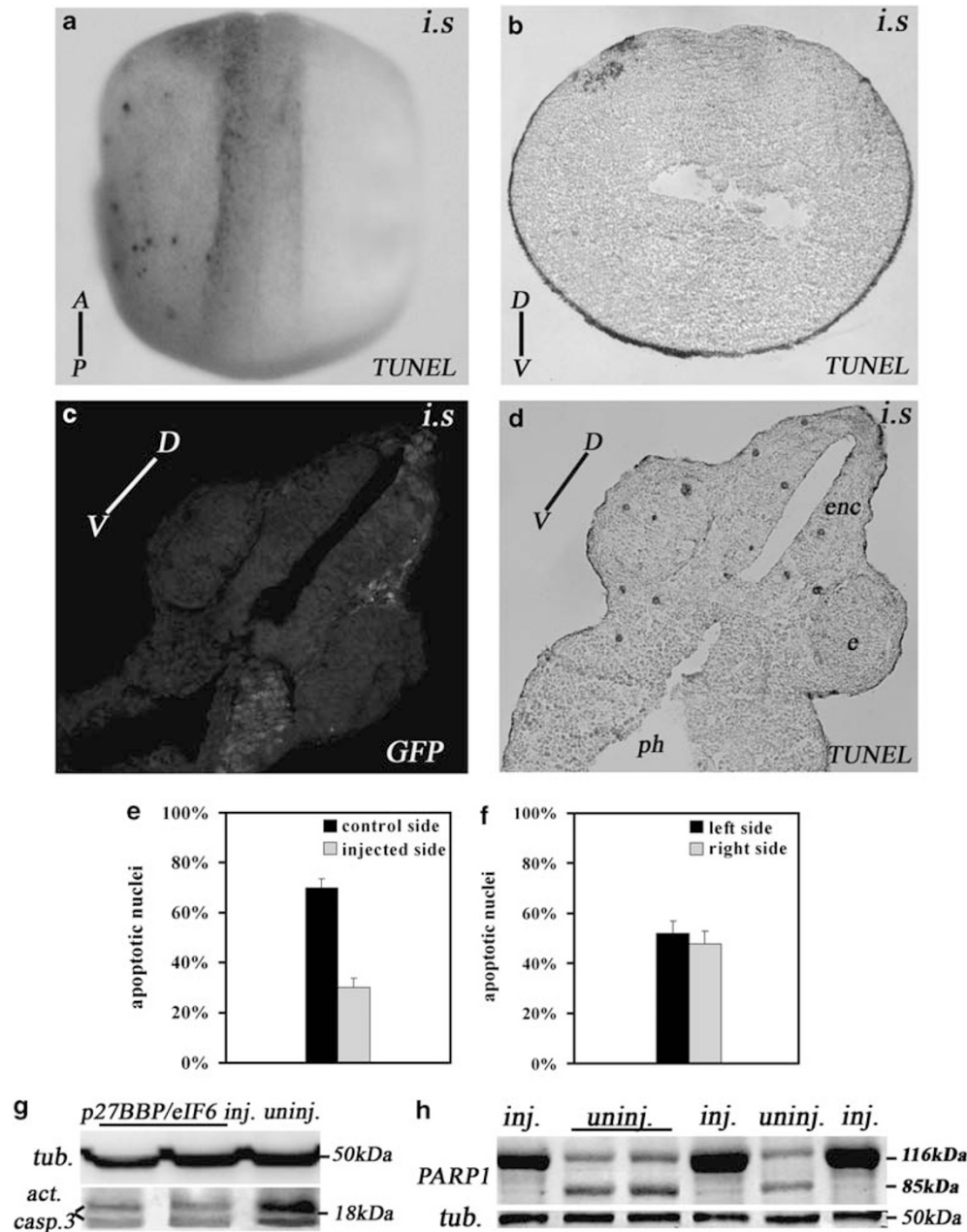
Figure 4 Apoptosis assays on embryos overexpressing Xp27^{BBP}/eIF6. (**a**) Whole-mount TUNEL staining was performed on Xp27^{BBP}/eIF6-injected st.19 embryo (neural plate stage). (**b**) Cross paraffin section taken from the anteriormost part of the TUNEL-stained embryo showed in **a**. (**c**) st.28 embryo overexpressing Xp27^{BBP}/eIF6, as observed by anti-GFP staining. (**d**) TUNEL staining on section of same embryo. Enc, encephalon; e, eye; ph, pharynx. The injected side showed less apoptosis compared with the control side, as counted in (**e**). Differences between injected and control sides are statistically significant ($n = 30$, $P < 0.05$). (**f**) TUNEL-labeled nuclei were counted in uninjected embryos and no significant difference in apoptotic nuclei was observed between the left and right sides ($n = 15$, $P < 0.05$). In the ordinates of panels **e** and **f** histograms, as well as in histograms of subsequent figures, the percentages are reported of apoptotic cells with respect to the total number of counted apoptotic cells (100%). (**g** and **h**) Western blots of st.28 Xp27^{BBP}/eIF6-injected and uninjected embryos exposed to anti-active caspase 3 specific for the cleaved form (**g**) or to anti-PARP1 (**h**) antibodies. Xp27^{BBP}/eIF6 overexpressing embryos showed less active caspase 3 (18 kDa) and cleaved PARP1 (85 kDA) compared with the uninjected ones. Normalization was performed with an anti-α-tubulin antibody. In the caspase 3 western blot, the effect of Xp27^{BBP}/eIF6 was underestimated because lysates were used, deriving from experiments in which the injection was performed in one blastomere of stage 2 embryos, thereby containing both the injected and control sides. In the PARP1 western blots, lysates were used, deriving from the injection of one-cell embryo. A-P, antero-posterior axis; D-V, dorsoventral axis

phosphorylation in Ser235 through the RACK1–PKC pathway. S235A mutants impair RACK1/PKC-mediated phosphorylation.[6] We performed injections of p27^{BBP}/eIF6 single mutants (S235A or S91A) into one blastomere of two-cell-stage *Xenopus* embryos. The mutant's overexpression was confirmed by immunofluorescence or western blot analysis with anti-p27^{BBP}/eIF6 antibody (data not shown). When we injected S235A mRNA, the embryos did not show the bent phenotype ($n = 70$) (Figure 7a1), as for embryos injected uniquely with GFP (Figure 7a2). TUNEL assay and counts of
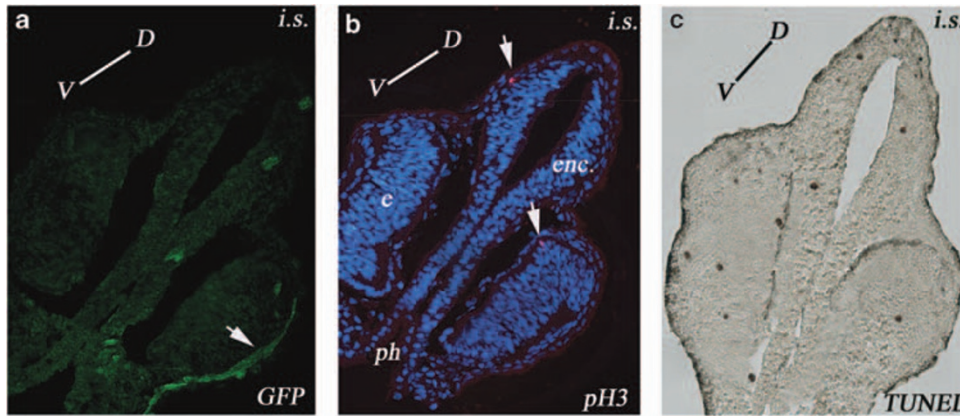
Figure 5 Embryos injected with Xp27[BBP]/eIF6 were treated with HUA at st.28 and the effects of such treatment on apoptosis were analyzed. (**a**) The injected side of the embryos is labeled with GFP (arrow). (**b**) Section of the same embryo as in panel **a** exposed to anti-pH3 and DAPI. The HUA treatment dramatically reduced anti-pH3 staining (arrows). Enc, encephalon; e, eye; ph, pharynx. (**c**) TUNEL staining showed a decrease in positive nuclei on the Xp27[BBP]/eIF6-injected side compared with the control side, indicating that apoptosis inhibition is independent from cell cycling. A-P, antero-posterior axis. The injected side is indicated (i.s)

apoptotic nuclei indicated no difference in apoptotic nuclei between the injected and control sides ($n = 30$, $P < 0.05$) (Figure 7c; data not shown).When we injected S91A mRNA, st.28 embryos showed the ring-shaped phenotype ($n = 90$) (Figure 7b) and a decrease in TUNEL-stained nuclei on the injected side ($n = 30$, $P < 0.05$) (Figure 7d; data not shown). We then carried out western blots to analyze caspase 3 activation and PARP1 cleavage in these samples. In S235A mRNA-injected-embryos, the levels of active caspase 3 and cleaved PARP1 were unaffected compared with uninjected embryos (Figures 7e and f). S91A mRNA-injected-embryos instead showed a decrease of active caspase 3 and cleaved PARP1 compared with uninjected and S235AmRNA-injected-embryos (Figures 7e and f).

Taken together, these results indicate that Ser 235 is the site responsible for the anti-apoptotic function of p27[BBP]/eIF6.

Xp27[BBP]/eIF6 regulation of Bcl-2/Bax levels. Members of the Bcl-2 family are key regulators in apoptosis, acting either as pro- or anti-apoptotic factors. Bcl-2 and Bax proteins are part of the core apoptotic machinery. At the functional level, Bcl-2 inhibits apoptosis whereas Bax promotes it, although the final decision of a cell to execute the cell death program depends on the balance among all the proteins of the apoptotic machinery.[27,28] In *X. laevis* early embryogenesis, Bcl-2 mRNA injection dramatically inhibits apoptosis, whereas Bax mRNA injection moderately promotes it.[29]

When we injected 300 pg of mRNA encoding Bcl-2 in one blastomere of two-cell-stage embryos, at st.28 these embryos showed the same ring-shaped phenotype as the one observed with Xp27[BBP]/eIF6 overexpression, being the external side of the embryos marked by GFP fluorescence (Figure 8a and b, embryos injected uniquely with GFP). TUNEL staining and counts of apoptotic nuclei showed that the Bcl-2 overexpression strongly inhibits apoptosis, as expected,[29] whereas pH3 immunofluorescence and counts of mitotic nuclei showed that proliferation is unaffected (data not shown).

To investigate whether p27[BBP]/eIF6 alters the level of endogenous Bcl-2 and Bax proteins, we carried out western blots, using anti-Bcl-2 and anti-Bax antibodies. Embryos overexpressing Bcl-2 showed an increase of Bcl-2 protein levels compared with uninjected embryos or embryos uniquely expressing GFP (Figure 8c), whereas Xp27[BBP]/eIF6 levels were unaffected (data not shown). Embryos overexpressing p27[BBP]/eIF6 also showed an increase of Bcl-2 but not of Bax protein levels, with respect to uninjected embryos (Figures 8c and d). In contrast, p27[BBP]/eIF6 morphants showed an increase of Bax but not of Bcl-2 protein levels compared with uninjected embryos or embryos expressing mispaired morpholino control (Figure 8e). Then, we carried out analysis of Bcl-2 and Bax mRNA levels in p27[BBP]/eIF6 overexpressors and morphants to investigate whether p27[BBP]/eIF6 similarly regulates Bcl-2/Bax expression. In Xp27[BBP]/eIF6-overexpressing embryos, the level of Bcl-2 mRNA increased, whereas the Bax level was unaffected. In morphants, an increase of Bax mRNA occurred, whereas Bcl-2 was unaffected (Figure 8f).

Further, we carried out experiments to rescue the p27[BBP]/eIF6-induced phenotype by co-injecting Xp27[BBP]/eIF6 mRNA (300 pg) and Bax mRNA (300 pg or 1 ng), together with the GFP mRNA (300 pg). The phenotypes of the injected embryos were not bent, similar to the embryos injected uniquely with GFP (Figure 9a). In addition, a small percentage (2–3%) of the injected embryos ($n = 60$) were bent with the concave, external side opposite to the injected side (Figure 9b). This phenotype was symmetrical to the phenotype obtained by Bcl-2 overexpression and identical to the phenotype obtained by p27[BBP]/eIF6 downregulation. Western blots using anti-p27[BBP]/eIF6 or anti-Myc antibodies on extracts of embryos injected with Xp27[BBP]/eIF6/bax mRNAs indicated that the embryos were successfully expressing both proteins (data not shown). pH3 immunofluorescence and counts of mitotic nuclei showed that Bax overexpression had no effects on cell proliferation (data not shown). TUNEL staining and counts of apoptotic nuclei showed that co-injection of Bax mRNA and Xp27[BBP]/eIF6 reversed the
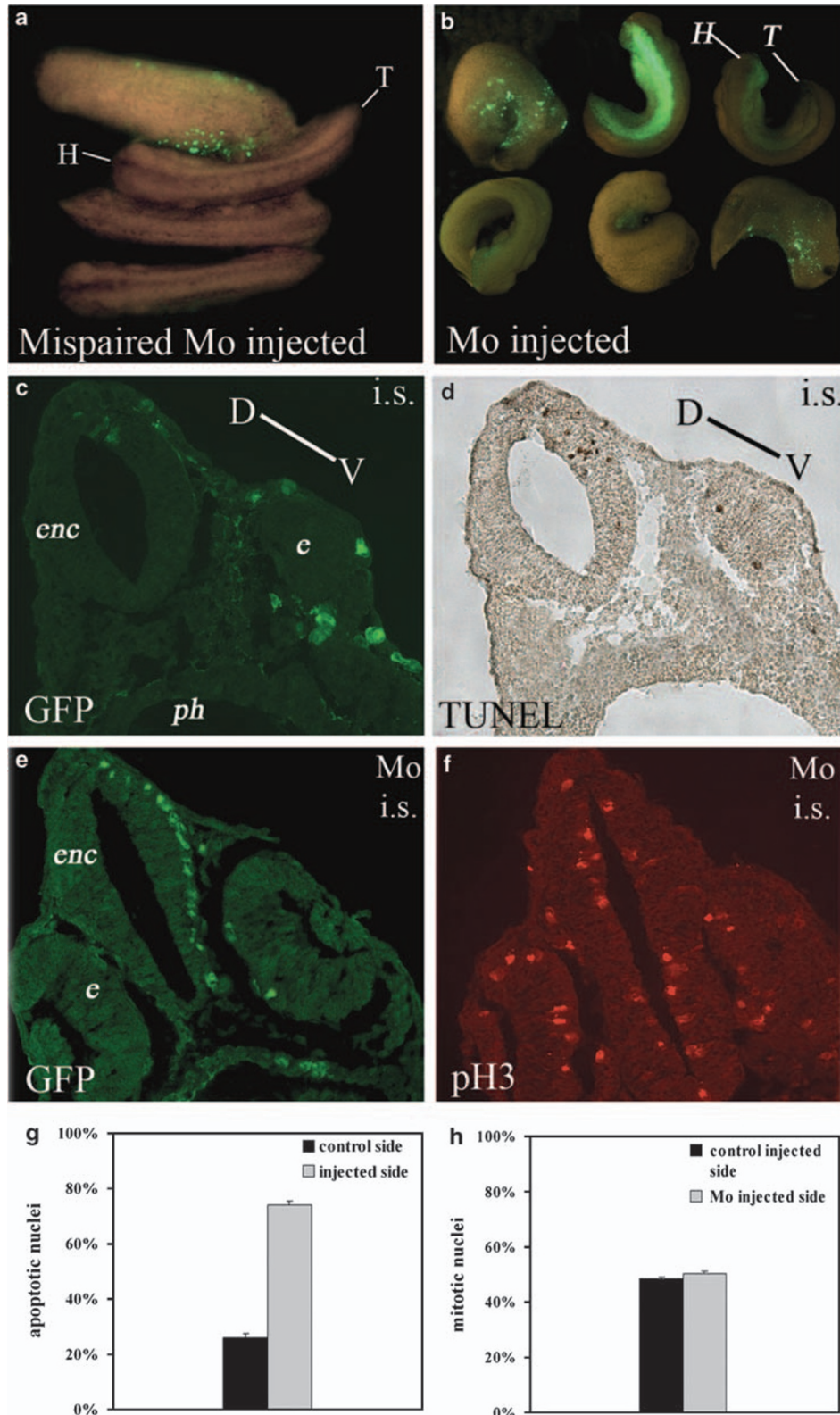
Figure 6 Effects of Xp27^{BBP}/eIF6 downregulation. (**a**) Control embryos injected with mispaired morpholino and GFP (lateral and dorsal views). (**b**) Morpholino-injected embryos have an inverted phenotype with respect to the one obtained by Xp27^{BBP}/eIF6 overexpression. In fact, the injected side marked by GFP fluorescence is the internal side of the bent embryo. (**c** and **d**) Sections of morpholino-injected embryo, in (**c**) GFP immunofluorescence on the injected side, in (**d** and **g**) TUNEL and counts of labeled nuclei. Apoptotic cells are more abundantly present on the injected side (i.s) ($n = 20$, $P < 0.05$). (**e** and **f**) Embryos injected with morpholino and GFP on one side (Mo i.s) and with mispaired morpholino on the opposite side. (**f** and **h**) Counts of pH3-positive nuclei show no difference in mitotic cells between the two sides of the embryo ($n = 20$, $P < 0.05$). H, head; T, tail; enc, encephalon; e, eye; ph, pharynx; D-V, dorsoventral axis
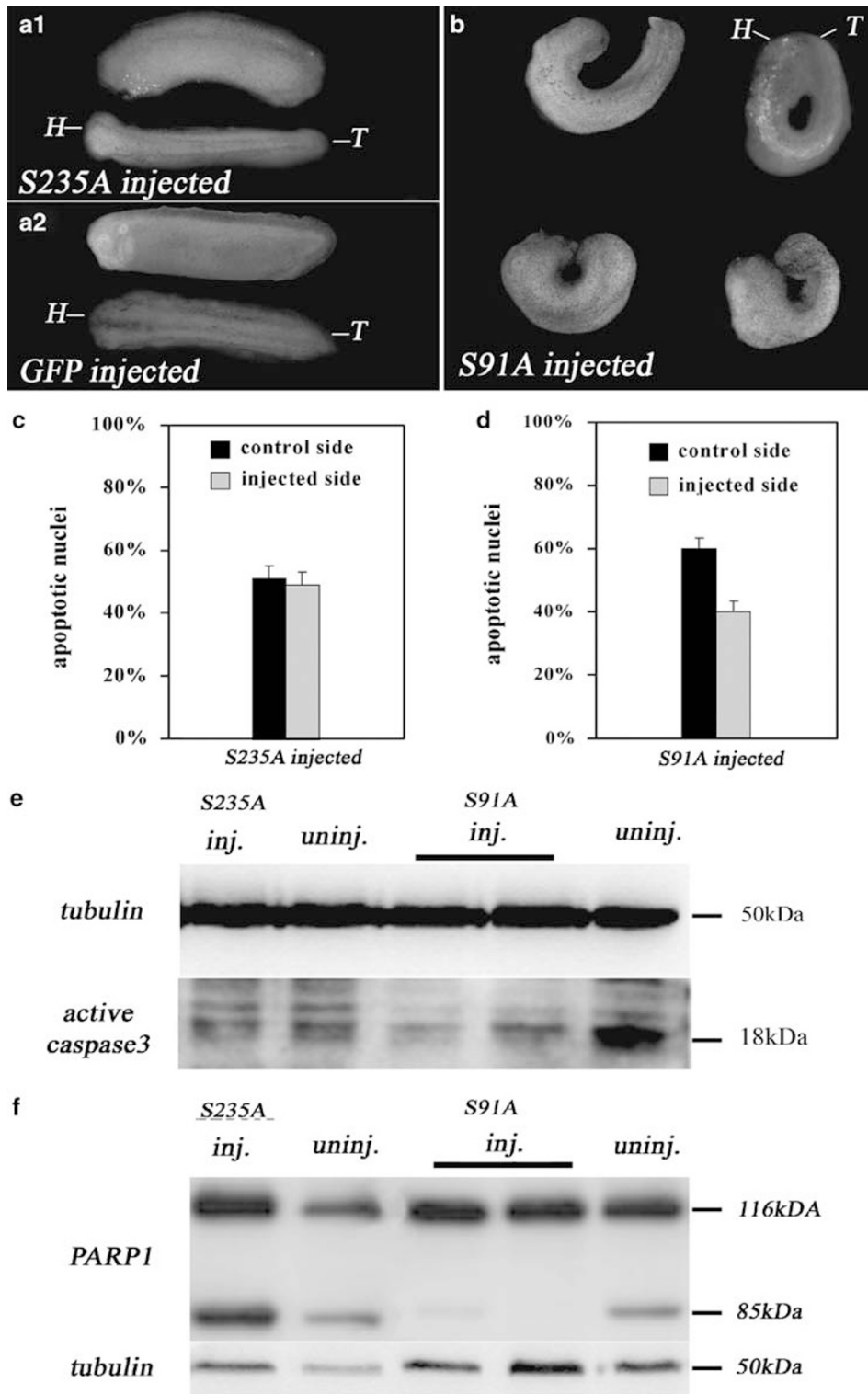
Figure 7 Effects of Xp27[BBP]/eIF6 mutant overexpression. (**a1**) S235A-injected embryos displaying non-bending as for embryos injected uniquely with GFP (**a2**) (lateral and dorsal views). (**b**) In all, 38% of S91A-injected embryos ($n = 90$) showed the curve-shaped phenotype as the one caused by Xp27[BBP]/eIF6 w.t. overexpression, with the external concave side marked by GFP. H, head; T, tail. (**c**) In S235A-injected embryos ($n = 70$), counts of TUNEL-positive nuclei indicate no difference in apoptosis between the injected and control sides ($n = 30$, $P < 0.05$). (**d**) TUNEL staining and counts of apoptotic nuclei showed a decrease in apoptosis on the injected side, compared with the control side ($n = 30$, $P < 0.05$). (**e**) S91AmRNA-injected embryos showed a decrease of active caspase 3 (18 kDa) compared with uninjected and S235A mRNA-injected embryos. (**f**) S91A-injected embryos showed more intact PARP1 compared with uninjected and S235-injected embryos. Normalization was performed with the anti-α-tubulin antibody. In the caspase 3 western blot, the effect of Xp27[BBP]/eIF6 was underestimated because lysates were used, deriving from experiments in which the injection was performed in one blastomere of stage 2 embryos, thus containing both the injected and control sides. In the PARP1 western blots, lysates were used, deriving from the injection of the one-cell embryo

inhibition of apoptosis produced by injecting Xp27[BBP]/eIF6 alone, as the number of apoptotic cells on the injected side was higher than on the uninjected side ($n = 30$, $P < 0.05$) (Figures 9c–e). When we co-injected the mRNA of S235A-mutated Xp27[BBP]/eIF6 with Bax mRNA, the number of embryos ($n = 48$) showing a symmetrical phenotype increased to 5 (data not shown). Altogether, these data indicate that Bax is able to reverse the anti-apoptotic

action of p27[BBP]/eIF6 and suggest that p27[BBP]/eIF6 acts upstream of Bcl-2/Bax machinery in apoptosis control.

Discussion

p27[BBP]/eIF6 function in regulating protein synthesis [6] may explain why it is abundant in growing or differentiating tissues. In fact, high expression of p27[BBP]/eIF6 is expected to occur according to the increased need of protein synthesis regulation along differentiation, cell growth and proliferation. Major expression of Xp27[BBP]/eIF6 was indeed observed during *X. laevis* embryonic development, in particular in the trunk region and in the brain.[8,9] Major expression of p27[BBP]/eIF6 is similarly reported for a variety of somatic cells (see Donadini *et al*.[10]). Moreover, a study by Sanvito *et al*.[11] showed that in cells progressing to malignancy, p27[BBP]/eIF6 is extremely overexpressed while being downregulated in tissues progressing to apoptosis.

Here, we studied a phenotype resulting from overexpressing Xp27[BBP]/eIF6 in *X. laevis* embryos and found that Xp27[BBP]/eIF6 is involved in protection from apoptosis, thus lending support to the predictions of Sanvito *et al*.[11] for cells progressing to apoptosis. We did not observe an increase in cell proliferation following p27[BBP]/eIF6 overexpression, implying that endogenous Xp27[BBP]/eIF6 suffices for cell cycle progression. In conditions of Xp27[BBP]/eIF6 downregulation, our mitosis assays in Xp27[BBP]/eIF6 morphants did not show differences in cell proliferation with respect to control conditions. The situation is different from what is observed in eIF6^{+/−} adult mice, where a decrease of 50% in the levels of all tissues was accompanied by a reduction in cell proliferation in the liver, fat cells and cultured fibroblasts.[5] The difference in these two observations may be due to several reasons: (i) the different way in which eIF6 was depleted, chronic in mice *versus* acute in *Xenopus*; (ii) different organs and time points analyzed; (iii) species-specific differences. It is, however, possible that eIF6 depletion may affect the translation of different classes of mRNA in different tissues, depending on the relative abundance of each mRNA, and that the phenotypic effects are the result of reaching thresholds that may vary among tissues.
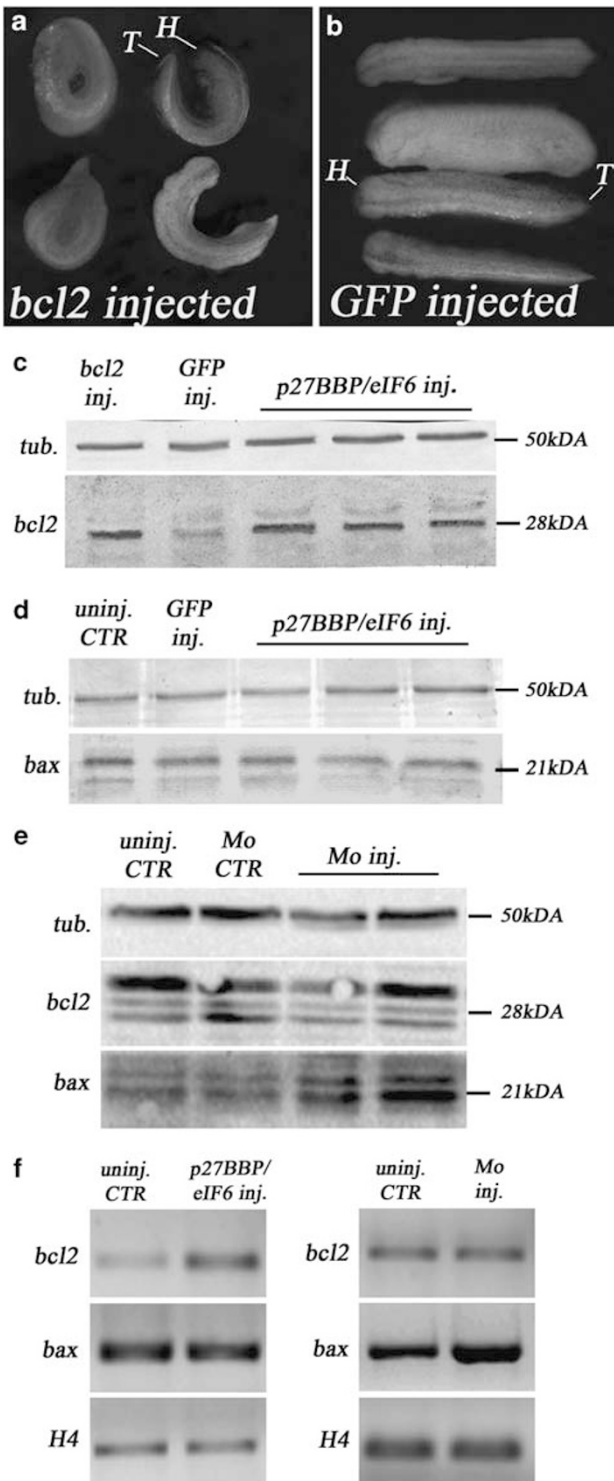
Figure 8 Effects of Xp27[BBP]/eIF6 on the Bcl-2/Bax levels. (**a**) In all, 50% of embryos unilaterally injected with Bcl-2 mRNA show at st.28 the same bent phenotype as the one caused by Xp27[BBP]/eIF6 overexpression, with the external side marked by GFP ($n = 60$). (**b**) Control embryos injected uniquely with GFP, lateral and dorsal views. (**b–e**) Western blots with anti-Bcl-2 or anti-Bax antibodies. Three sets of Xp27[BBP]/eIF6-injected embryos (st.28) were used in the blots in panels **c** and **d**. (**c**) Bcl-2 or Xp27[BBP]/eIF6-injected-embryos showed an increase of Bcl-2 protein compared with uninjected embryos. (**d**) The level of Bax was unaffected in embryos overexpressing Xp27[BBP]/eIF6, as well as in uninjected embryos. (**e**) Levels of Bcl-2 and Bax were analyzed in embryos injected with p27[BBP]/eIF6 morpholino or mispaired morpholino control. An increase of Bax but not of Bcl-2 protein levels was shown, compared with uninjected embryos or embryos expressing mispaired morpholino. Normalization was performed with the anti-α-tubulin antibody. (**f**) Analysis of Bcl-2 and Bax mRNA levels in p27[BBP]/eIF6 overexpressors and morphants, compared with levels in uninjected embryos. In Xp27[BBP]/eIF6-overexpressing embryos, the level of Bcl-2 mRNA increased, whereas the Bax mRNA level was unaffected. In morphants, an increase of Bax mRNA occurred, whereas Bcl-2 mRNA was unaffected. Normalization was performed using H4 primers. These data underestimate the effect of Xp27[BBP]/eIF6 because entire embryos were used for the blots and RT-PCR preparation
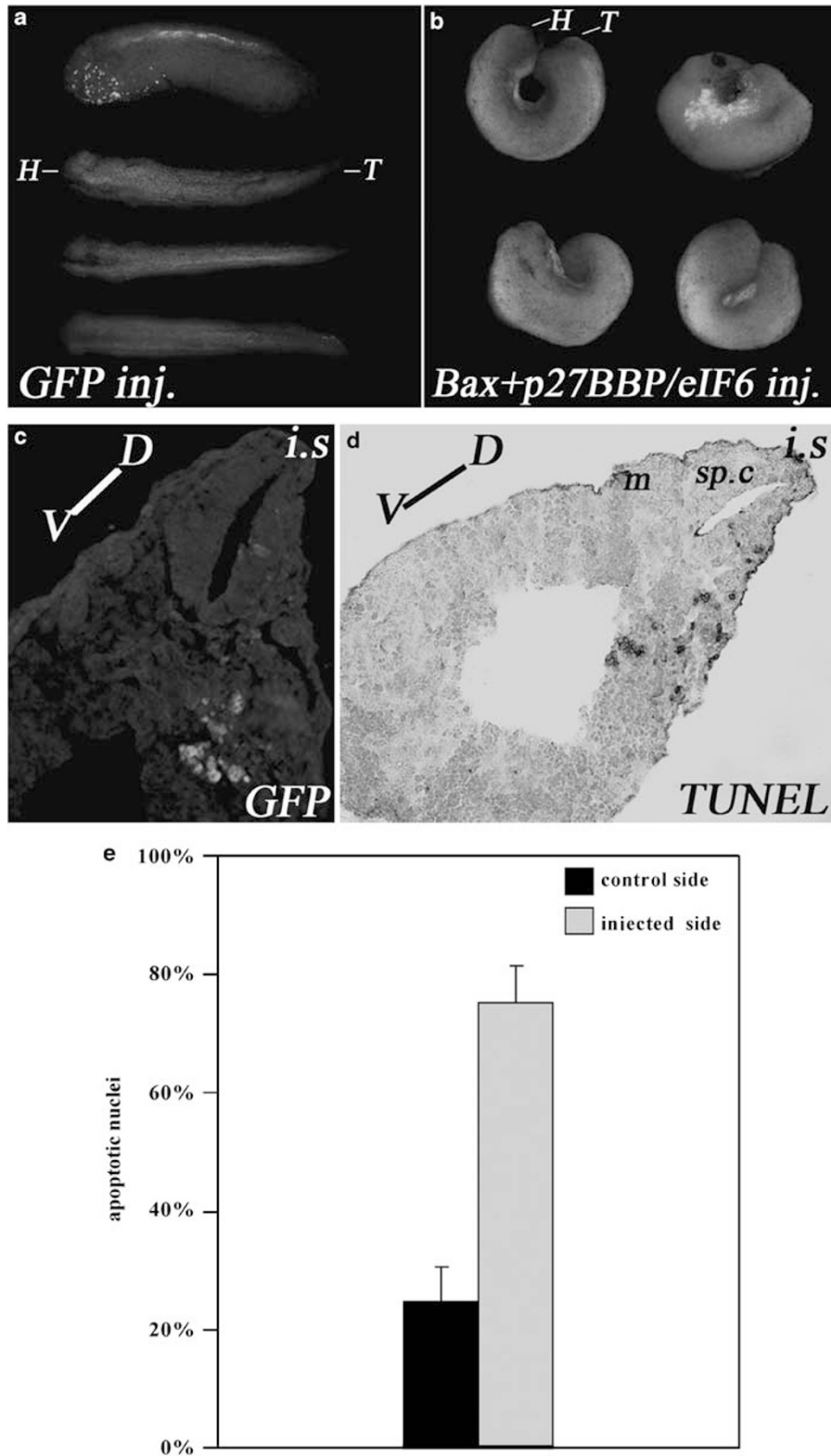
Figure 9 Bcl-2-associated X protein (Bax) rescues embryos injected with Xp27^BBP/eIF6. (**a**) Control embryos injected uniquely with GFP (lateral and dorsal views). Embryos ($n = 60$) co-injected in one blastomere at two-cell stage with Xp27^BBP/eIF6 and Bax are not curved, yet in 2–3% of the co-injected embryos, an inverted phenotype with respect to the one obtained by injecting only Xp27^BBP/eIF6 is observed. The embryos were bent, but the external side originated from the uninjected blastomere (**b**). H, head; T, tail. (**c–e**) On the injected side, marked by GFP (**c**), TUNEL staining (**d**) and counts (**e**) showed that the labeled apoptotic nuclei are more abundant on the injected side, compared with the control side ($n = 30$, $P < 0.05$). m, miotome; sp.c., spinal cord; A-P, antero-posterior axis. The injected side is indicated (i.s)

In many vertebrates, apoptosis is needed for the correct development of embryonic structures of several organisms, both at the beginning of embryogenesis and in the morphogenesis of anlagen, such as the limb and kidney, as well as the nervous system.[30,31] In *X. laevis*, apoptosis is active in the embryo starting at the beginning of gastrulation and its spatio-temporal pattern has been thoroughly described until the tadpole stage.[20] Cell death and cell survival are regulated by complex and interacting signals. Data by Finkielstein *et al*.[32] and Yeo and Gautier [17] have indicated that, in *X. laevis*, after MBT, Bcl-2 and Bax balance and downstream caspase activation are the main mechanisms involved in the control of apoptosis. These step-by-step controlled mechanisms converge eventually to a yes-or-no result that can be experimentally reverted. Accordingly, our data indicate that Xp27^BBP/eIF6 overexpression is able to shift the program of cell death to cell survival, as shown by TUNEL staining, caspase 3 activation and PARP1 cleavage. Consistently, p27^BBP/eIF6 loss-of-function experiments elicit an increase in apoptosis accompanied by reversal of the phenotype. By overexpressing the mRNA of the anti-apoptotic factor Bcl-2, a bent phenotype was found as in the embryos injected with Xp27^BBP/eIF6 mRNA, and consistent differences in apoptotic cell number were detected between the injected and uninjected sides of the embryos. Xp27^BBP/eIF6 appears to be upstream in the Bcl-2 apoptotic pathway because Xp27^BBP/eIF6 overexpressing embryos show an increase of Bcl-2 mRNA and protein, which does not occur in Xp27^BBP/eIF6 morphants. Consistently, although Xp27^BBP/eIF6 over-expressing embryos do not increase Bax expression, Xp27^BBP/eIF6 morphants have higher levels of Bax mRNA and protein. When Bax mRNA was co-injected with Xp27^BBP/eIF6 mRNA, the bent phenotype recovered and a low occurrence was observed of the reverted phenotype, the same phenotype obtained in Xp27^BBP/eIF6 downregulation experiments. We reasoned that this result is a compromise balance between the anti-apoptotic action of Xp27^BBP/eIF6 and the pro-apoptotic action of Bax. In favor of this hypothesis, when mutated Xp27^BBP/eIF6 mRNA (lacking anti-apoptotic function) was co-injected with Bax, the number of embryos with reverted phenotypes increased. Altogether, these data indicate that p27^BBP/eIF6 may act by shifting the balance between pro- and anti-apoptotic factors in favor of cell survival and strongly suggest that Xp27^BBP/eIF6 acts through an upstream, yet unknown, regulator of the Bcl-2/Bax balance. Moreover, in Xp27^BBP/eIF6 overexpressors, the decrease in apoptosis also occurred when the cell cycle was stopped, following HUA exposure, indicating that the reduction in apoptosis levels was independent from cell cycling as in untreated *Xenopus* embryos.[17]

In mammalian cultured cells, on PKC phosphorylation on serine 235, p27^BBP/eIF6 is released from 60S, the 80S forms and translation is started, whereas the S235 mutant binds the 60S but cannot be released.[6] In a lentiviral rescue experiment, the S235 mutant did not recover translation downstream of the growth factors, whereas the w.t. did.[5] Together, the data suggested that the regulated release of p27^BBP/eIF6 from 60S positively affects translation, whereas the mutant does not. In other terms, the current understanding is that the regulated anti-association activity of w.t. p27^BBP/eIF6

may positively affect translation, whereas the S235 mutant does not. Yet it is not known whether p27^BBP/eIF6 anti-association activity equally affects the translation of all mRNAs or is somewhat selective. Two potential PKC phosphorylation sites are present in Xp27^BBP/eIF6 cDNA, that is, 235 SmR as in mammals and 91SvR typical of *X. laevis*.[8,9] In *X. laevis*, we also know that p27^BBP/eIF6 is associated with 60S polysome fractions and that a serine phosphorylated isoform of p27^BBP/eIF6, consequent on PKC phosphorylation, is present all along embryogenesis. This finding suggests a highly conserved function of Xp27^BBP/eIF6, depending on phosphorylation, in regulating the availability of active ribosomes to the translation machinery.[7] Therefore, in our trials, it appeared of special interest to learn which of the two potential sites of Xp27^BBP/eIF6 phosphorylation was responsible for the anti-apoptotic function of Xp27^BBP/eIF6. Our data indicate that the site is serine 235 SmR. In fact, it is on injection of the 235 SmR mutant, and not of the 91SvR mutant, that straight st.28 embryos are obtained, in contrast to the bent phenotype obtained by injection of Xp27^BBP/eIF6 w.t. Our data suggest that the anti-apoptotic function of Xp27^BBP/eIF6 depends on its role in regulating protein synthesis, if we correctly hypothesize that also in *X. laevis* the 235 SmR site is PKC-phosphorylated to allow joining of the 40S–60S subunits. In other words, the specific role of w.t. Xp27^BBP/eIF6 in favoring cell survival would require that its proper function be that of a regulator of protein synthesis affecting the translation of mRNAs involved in apoptosis, in contrast to the S235 mutant. Xp27^BBP/eIF6 seems to be part of a mechanism acting at translation and reverting cell death to cell survival, thus regulating the apoptotic process during normal development and giving way to a new interpretation for the major presence of this protein in embryonic anlagen. In particular, considering the conditions that our Xp27^BBP/eIF6 gain-of-function and loss-of-function experiments brought to a specific regulation of the Bcl-2/Bax levels, it will be important to establish the nature of the factor(s) regulating this balance and the involvement of p27^BBP/eIF6 in regulating its translation.

Materials and Methods

Animals. Adult *X. laevis* females were obtained from 'Rettili' (Varese, Italy). They were kept and used at the Department of Structural and Functional Biology, the University of Naples, Federico II, according to the guidelines and policies dictated by the University Animal Welfare Office and in agreement with European Community laws.

To obtain eggs, *X. laevis* females were injected in the dorsal lymphatic sac with 500 units of Gonase (AMSA, Rome, Italy) in Amphibian Ringer (111 mM NaCl, 1.3 mM CaCl2, 2 mM KCl, 0.8 mM MgSO4, 25 mM *N*-2-hydroxyethylpiperazine-*N'*-2-ethanesulfonic acid (HEPES), pH 7.8). Fertilized eggs and embryos were obtained by standard insemination methods and staged according to Nieuwkoop and Faber.[33]

Microinjections. To generate pCS2p27^BBP/eIF6, the cDNA cloned in pDrive[8,9] was subcloned into the *BamHI/XhoI* sites of the pCS2 + vector. The complete coding sequence of XBcl-2 was obtained by reverse transcriptase (RT)-PCR, using the primers forward: 5′-ACAATGGAGGGCAGCAGTAG-3′ and reverse: 5′-TTGC AGAACTTCCTGGGTGT-3′, on the basis of the sequence of the *Xenopus* homolog of Bcl-2, XR11 (Accession Nos. X82461). The PCR products were cloned into the pCRII vector (Invitrogen, Life Technologies, Carlsbad, CA, USA) and subsequently subcloned into the *BamHI/XhoI* sites of the pCS2 + vector. The full-length clone was

completely sequenced. The pCS2MTXBax plasmid was kindly offered by JL Maller (University of Colorado, School of Medicine, USA).

Capped synthetic RNAs were generated by *in vitro* transcription using the Sp6 Message Machine kit (Ambion, Austin, TX, USA).

The p27[BBP]/eIF6 antisense morpholino used was 5′-GCGGACGGCCATGTTGG CTTCTTAG-3′ (Gene Tools LLC, Philomath, OR, USA). The mispaired morpholino control used was 5′-GCcGACcGCCATcTTGcCTTCTaAG-3′ (Gene Tools LLC). pCS2MTGFP mRNA was always co-injected to label the injected side.

RNAs were injected into the animal hemisphere of a single cell of one- and two-cell embryos using a Drummond 'Nanoject' apparatus (Drummond "Nanoject II" Cat.N.3-000-204). The amounts injected ranged between 100 pg to 1 ng, in most cases 200–300 pg. In particular, for samples destined to western blots of Parp1, injection were performed in one-cell embryos using 500 pg Xp27[BBP]/eIF6 to better visualize the difference in Parp1 cleavage between injected and uninjected embryos. During injection, embryos were cultured in 3% Ficoll in 0.1% Ringer. The phenotype of the injected embryos was scored when the uninjected embryos reached stage 28. The samples were photographed at the Leica MZ16F UV stereomicroscope, equipped with a Leica DFC 300Fx camera and IM50 image manager software.

RNA extraction and RT-PCR. Total RNA was extracted from st.19 embryos using Tri Reagent (Sigma, St Louis, MO, USA) according to the manufacturer's recommendations. RT-PCR was carried out using the Super Script VILO cDNA synthesis kit (Invitrogen, Carlsbad, CA, USA) and primers to detect Bcl-2 (forward: 5′-ACAATGGAGGGCAGCAGTAG-3′ and reverse: 5′-TTGCAGAACTTCCTGG GTGT-3′), Bax (forward: 5′-AGGCATCTCCCAACAGAGTG-3′ and reverse: 5′-C TTCCAGATGGCAAGAGAGG-3′) or H4 (forward: 5′-CGGGATAACATTCAGG GTA-3′ and reverse: TCCATGGCGGTAACTGTC-3′).

PCR site-directed mutagenesis. Site-directed mutagenesis to generate S235A and S91A was performed as in De Marco *et al*.[34] The following oligo- nucleotides were used to introduce the S235A mutation into pCS2p27[BBP]/eIF6 wild type: 5′-CCTAGTACTATTGCCACCGCCATGAGGGGCTCCCTC-3′ and 5′-GAGG GAGCCCCTCATGGCGGTGGCAATAGTACTAGG-3′. The following oligonucleotides were used to introduce the S91A mutation into pCS2 p27[BBP]/eIF6 wild type: 5′-GAA ACAGCTTGCCCGACGCCGTGCGAATTCAGAGAG-3′ and 5′-CTCTCTGAATTCGC ACGGCGTCGGGCAAGCTGTTTC-3′.

The DNA sequence of the mutants was confirmed by sequence analysis.

Sample preparation for SDS-PAGE and western blot. Embryos were homogenized in HEPES buffer pH 7.5 containing 900 mM glycerol, 0.02 mM NaN3, 1 mM DTT, 1 mM ATP, 5 mM ethylene glycol tetraacetic acid (EGTA) (buffer I) and the following protease inhibitors (Sigma): 2 mM $N\alpha$-(*p*-toluene sulfonyl)-L-arginine methyl ester (TAME), 5 mg/ml soybean trypsin inhibitor (SBTI), 5 μg/ml aprotinin and 10 μM E64. Protein concentration was determined in the supernatants following centrifugation (15 000 × g for 40 min at 4 °C) with the BCA protein assay reagent (Pierce, Rockford, IL, USA). After boiling in sample buffer with 1 mM DTT, aliquots of 40 μg of proteins were analyzed through SDS-polyacrylamide gel electrophoresis (PAGE) 8% or 15% polyacrylamide using standard Tris glycine buffer and using molecular mass standards (200, 116, 97, 45, 31, 21 or 14 kDa) (Bio-rad, Hercules, CA, USA). Western blotting on nitrocellulose membrane was carried out as in Maturi *et al*.[35] Incubation with the antibodies was carried out using an anti-p27[BBP]/eIF6 antibody (1 : 1000 dilution v/v),[1] rabbit anti-Caspase 3 Active, specific for the cleaved form of caspase (1 : 400 dilution, v/v) (Sigma C8487), mouse anti-α-tubulin (1 : 500 dilution, v/v) (Sigma), anti-PARP H-250 polyclonal antibody (1 : 500 dilution, v/v) (Santa Cruz Biotechnology, Heidelberg, Germany), anti-Bcl-2 monoclonal antibody (1 : 250 dilution, v/v) (Santa Cruz Biotechnology) and polyclonal anti-Bax (1 : 200 dilution, v/v) (Calbiochem, Darmstadt, Germany). Antibody binding was detected with secondary anti-mouse or anti-rabbit IgGs coupled with horseradish peroxidase (Pierce) and revealed with the enhanced chemiluminescence kit (Pierce).

BrdU and HUA experiments. Xp27[BBP]/eIF6 overexpressing embryos were injected at st.28 with BrdU (Roche, Mannheim, Germany) in the gut, fixed 2 h later and cryostat-sectioned. Preliminary experiments showed that at this stage cell division occurs in a few minutes (see also Viczian *et al*.[19]). Sections were washed with 2 N HCl for 45 min and then neutralized with several phosphate-buffered saline (PBS) washes. The mouse anti-BrdU antibody (Sigma) was added at 1 : 500 dilution and the sections were incubated at 4 °C overnight. Staining was completed by incubation with BODIPY FL goat anti-mouse IgG (Invitrogen). To block DNA synthesis, embryos were incubated in a solution of 20 mM HUA (Sigma) and

150 μM aphidicolin (Sigma) in 0.1 × Ringer as described in Harris and Hartenstein.[24] Aphidicolin was diluted from 10 mg/ml stock in dimethyl sulfoxide. Embryos were kept in HUA at 16 °C for 5 h until fixation.

TUNEL staining. TUNEL staining for the identification of apoptotic cells was carried out using the ApopTag Peroxidase *In situ* Apoptosis Detection Kit (Chemicon International, Inc., Temecula, CA, USA) in accordance with the manufacturer's instructions. Counts of TUNEL-positive nuclei in sections of fixed embryos were reported in histograms in which the ordinates indicate percentages of apoptotic cells with respect to the total number of counted apoptotic cells (100%). The data were statistically validated by PAIRED *t*-test analysis.

The whole-mount TUNEL staining protocol was performed as described in Hensey and Gautier.[16] Detection and chromogenic reaction was carried out as in Harland.[36] The embryos were blocked in 20% goat serum, followed by incubation with the anti-digoxigenin antibody coupled to alkaline phosphatase (Roche). Staining was developed using BM-purple (Roche). Embryos were viewed following dehydration in methanol and mounting in benzyl benzoate/benzyl alcohol 2 : 1. Whole mounts were photographed at the Leica MZ 16F. Some embryos were cleared, paraffin-embedded and sectioned.

Immunofluorescence. *X. laevis* embryos were fixed in 4% formaldehyde at 4 °C and stored in 100% methanol at −20 °C. Frozen sections of 10-μm thickness were obtained for immunofluorescence after embedding and freezing in Killik (Bio Optica, Milan, Italy). Nonspecific background was blocked by incubating the sections for 30 min in normal goat serum 3% in PBS, 0.5% BSA, 0.1% Tween before exposure to O/N at 4 °C to rabbit anti-p27[BBP]/eIF6,[1,7] rabbit anti-GFP (Molecular Probe, Milan, Molecular probes-Invitrogen) or to polyclonal anti-pH3 antibody (UPSTATE, Lake Placid, NY, USA), diluted 1 : 500 in PBS containing 0.5% BSA and 0.1% Tween. Staining was completed by incubating the samples with anti-rabbit goat IgG BODIPY FL-conjugated or Texas-Red-conjugated (Molecular Probe), followed by nuclei counterstaining with DAPI and mounting in PBS/glycerol (9 : 1, v/v). Sections were observed and photographed using a Leica CTR 6500 UV microscope equipped with a Leica application suite.

The number of anti-pH3-positive nuclei counted in sections of fixed embryos was reported in histograms in which the ordinates indicate percentages of labeled cells with respect to the total number of labeled cells (100%) counted in an embryo entirely sectioned. All the data are statistically validated by PAIRED *t*-test analysis.

Immunohistochemistry. Whole-mount antibody staining was performed following standard procedures for indirect immunohistochemistry using an anti- muscle ATPase monoclonal antibody 12/101 at 1 : 10 dilution. This antibody was developed by Dr JP Brockes (Department of Biochemistry and Molecular Biology, University College London, London, UK), obtained from the Developmental Studies Hybridoma Bank (under the auspices of the National Institute of Child Health and Human Development, NIH) and maintained at the University of Iowa, Department of Biological Sciences, Iowa City, IA, USA. The protocol was completed by incubating the samples with the biotinylated secondary antibody and the avidin-biotinylated peroxidase complex (Vector Laboratories, Inc, Burlingame, CA, USA). The reaction product was visualized by incubation in diaminobenzidine (Vector Laboratories).

1. Biffo S, Sanvito F, Costa S, Preve L, Pignatelli R, Spinardi L *et al*. Isolation of a novel β4 integrin binding protein (p27[BBP]) highly expressed in epithelial cells. *J Biol Chem* 1997; **272**: 30314–30321.
2. Basu U, Si K, Warner JR, Maitra U. The Saccharomyces cerevisiae TIF6 gene encoding translation initiation factor 6 is required for 60S ribosomal subunit biogenesis. *Mol Cell Biol* 2001; **21**: 1453–1462.
3. Senger B, Lafontaine DL, Graindorge JS, Gadal O, Camasses A, Sanni A *et al*. The nucleolar Tif6p and Efl1p are required for a late cytoplasmic step of ribosome synthesis. *Mol Cell* 2001; **8**: 1363–1373.

4. Sanvito F, Piatti S, Villa A, Bossi M, Lucchini G, Marchisio PC *et al.* The beta4 integrin interactor p27(BBP/eIF6) is an essential nuclear matrix protein involved in 60S ribosomal subunit assembly. *J Cell Biol* 1999; **144**: 823–837.

5. Gandin V, Miluzio A, Barbieri A, Magri L, Kiyokawa H, Marchisio PC. eIF6 is rate limiting for translation, growth and transformation. *Nature* 2008; **455**: 684–688.

6. Ceci M, Gaviraghi C, Gorrini C, Sala LA, Offenhauser N, Marchisio PC *et al.* Release of eIF6 (p27^BBP) from the 6OS subunit allows 80S ribosome assembly. *Nature* 2003; **426**: 579–584.

7. Carotenuto R, De Marco N, Biffo S, Wilding M, Vaccaro MC, Marchisio PC *et al.* Phosphorylation of p27^BBP/eIF6 and its association with the cytoskeleton are developmentally regulated in Xenopus oogenesis. *Cell Mol Life Sci* 2005; **62**: 1641–1652.

8. Vaccaro MC, Cuccaro M, De Marco N, Campanella C. Isolation and expression pattern of p27 ^BBP/eIF6 cDNA in Xenopus laevis embryos. *Mol Reprod Dev* 2006a; **73**: 485–490.

9. Vaccaro MC, Cuccaro M, De Marco N, Campanella C. Isolation and expression pattern of p27 ^BBP/eIF6 cDNA in Xenopus laevis embryos ERRATUM *Mol Reprod Dev* 2006b; **73**:1612.

10. Donadini A, Giodini A, Sanvito F, Marchisio PC, Biffo S. The human ITGB4BP gene is constitutively expressed *in vitro*, but highly modulated *in vivo*. *Gene* 2001; **266**: 35–43.

11. Sanvito F, Vivoli F, Gambini S, Santambrogio G, Catena M, Viale E *et al.* Expression of a highly conserved protein, p27^BBP, during the progression of human colorectal cancer. *Cancer Res* 2000; **60**: 510–516.

12. Vreugde S, Ferrai C, Miluzio A, Hauben E, Marchisio PC, Crippa M *et al.* Nuclear myosin VI enhances RNA polymerase II dependent transcription. *Mol Cell* 2006; **23**: 749–755.

13. Ji Y, Shah S, Soanes K, Islam MN, Hoxter B, Biffo S *et al.* Eukaryotic initiation factors 6 selectively regulates Wnt signalling and β-catenin protein synthesis. *Oncogene* 2008; **27**: 755–762.

14. Chendrimada TP, Finn KJ, Ji X, Baillat D, Gregory RI, Liebhaber SA *et al.* MicroRNA silencing through RISC recruitment of eIF6. *Nature* 2007; **447**: 823–829.

15. Eulalio A, Huntzinger E, Izaurralde E. GW182 interaction with Argonaute is essential for miRNA-mediated translation repression and mRNA decay. *Nat Struct Mol Biol* 2008; **15**: 346–353.

16. Hensey C, Gautier J. A developmental timer that regulates apoptosis at the onset of gastrulation. *Mech Dev* 1997; **69**: 183–195.

17. Yeo W, Gautier J. A role for programmed cell death during early neurogenesis in Xenopus. *Dev Biol* 2003; **260**: 31–45.

18. Jacobson MD, Weil M, Raff MC. Programmed cell death in animal development. *Cell* 1997; **88**: 347–354.

19. Viczian AS, Vignali R, Zuber ME, Barsacchi G, Harris WA. Xotx5b and Xotx2 regulate photoreceptor and bipolar fates in the Xenopus retina. *Development* 2003; **130**: 1281–1294.

20. Hensey C, Gautier J. Programmed cell death during xenopus development: a spatio-temporal analysis. *Dev Biol* 1998; **238**: 36–48.

21. Gavrieli Y, Sherman Y, Ben-Sasson SA. Identification of programmed cell death *in situ* via specific labeling of nuclear DNA fragmentation. *J Cell Biol* 1992; **119**: 493–501.

22. Kaufmann SH, Lee SH, Meng XW, Loegering DA, Kottke TJ, Henzing AJ *et al.* Apoptosis-associated caspase activation assays. *Methods* 2008; **44**: 262–272.

23. Yuan J, Shaham S, Ledoux S, Ellis HM, Horvitz HR. The C. elegans cell death gene ced-3 encodes a protein similar to mammalian interleukin-1 beta-converting enzyme. *Cell* 1993; **75**: 641–652.

24. Harris WA, Hartenstein V. Neuronal determination without cell division in Xenopus embryos. *Neuron* 1991; **6**: 499–515.

25. Zorn AM, Mason J. Gene expression in the embryonic Xenopus liver. *Mech Dev* 2001; **103**: 153–157.

26. Rot-Nikcevic I, Wassersug RJ. Arrested development in Xenopus laevis tadpoles: how size constrains metamorphosis. *J Exp Biol* 2004; **207**: 2133–2144.

27. Adams JM, Cory S. Life-or-death decisions by the Bcl-2 protein family. *Trends Biochem Sci* 2001; **26**: 61–66.

28. Cory S, Adams JM. The Bcl2 family: regulators of the cellular life-or-death switch. *Nat Rev Cancer* 2002; **2**: 647–656.

29. Tríbulo C, Aybar MJ, Sánchez SS, Mayor R. A balance between the anti-apoptotic activity of Slug and the apoptotic activity of msx1 is required for the proper development of the neural crest. *Dev Biol* 2004; **275**: 325–342.

30. Coles HS, Burne JF, Raff MC. Large-scale normal cell death in the developing rat kidney and its reduction by epidermal growth factor. *Development* 1993; **118**: 777–784.

31. Burek MJ, Oppenheim RW. Programmed cell death in the developing nervous system. *Brain Pathos* 1996; **6**: 427–446.

32. Finkielstein CV, Lewellyn AL, Maller JL. The midblastula transition in Xenopus embryos activates multiple pathways to prevent apoptosis in response to DNA damage. *Proc Natl Acad Sci USA* 2001; **98**: 1006–1011.

33. Nieuwkoop PD, Faber J. *Normal Table of Xenopus laevis.* Daudin, Amsterdam: North Holland, 1967.

34. De Marco N, Buono M, Troise F, Diez-Roux G. Optineurin increases cell survival and translocates to the nucleus in a Rab8-dependent manner upon an apoptotic stimulus. *J Biol Chem* 2006; **281**: 16147–16156.

35. Maturi G, Infante V, Carotenuto R, Focarelli R, Caputo M, Campanella C. Specific gly-coconjugates are present at the oolemma of the fertilization site in the egg of Discoglossus pictus (Anurans) and bind spermatozoa in an *in vitro* assay. *Dev Biol* 1998; **204**: 210–223.

36. Harland RM. *In situ* hybridisation: an improved whole mount method for Xenopus embryos. *Meth Cell Biol* 1991; **36**: 675–685.